The Astrophysical Journal, 976:227 (8pp), 2024 December 1 https://doi.org/10.3847/1538-4357/ad8d5b

The Excess of JWST Bright Galaxies: A Possible Origin in the Ground State of Dynamical Dark Energy in the Light of DESI 2024 Data

N. Menci[1], A. A. Sen[2], and M. Castellano[1]
[1] INAF—Osservatorio Astronomico di Roma, via Frascati 33, I-00078 Monte Porzio, Italy
[2] Centre For Theoretical Physics, Jamia Millia Islamia, New Delhi, 110025, India
Received 2024 July 11; revised 2024 October 23; accepted 2024 October 29; published 2024 November 26

Abstract

Recent observations by JWST yield a large abundance of luminous galaxies at $z \gtrsim 10$ compared to that expected in the ΛCDM scenario based on extrapolations of the star formation efficiency measured at lower redshifts. While several astrophysical processes can be responsible for such observations, here we explore to what extent such an effect can be rooted in the assumed dark energy (DE) sector of the current cosmological model. This is motivated by recent results from different cosmological probes combined with the last data release of the Dark Energy Spectroscopic Instrument, which indicate a tension in the DE sector of the concordance ΛCDM model. We have considered the effect of assuming a DE characterized by a negative Λ as the ground state of a quintessence field on the galaxy luminosity function at high redshifts. We find that such models naturally affect the galaxy UV luminosities in the redshift range $10 \lesssim z \lesssim 15$ needed to match the JWST observations, and with the value of $\Omega_\Lambda = [-0.6, -0.3]$ remarkably consistent with that required by independent cosmological probes. A sharp prediction of such models is the steep decline of the abundance of bright galaxies in the redshift range $15 \lesssim z \lesssim 16$.

Unified Astronomy Thesaurus concepts: Cosmological parameters (339); Cosmological models (337); Dark energy (351); Quintessence (1323); Galaxy formation (595)

1. Introduction

The large number density of UV-bright galaxies measured by JWST at redshift $z \gtrsim 9$ appreciably exceeds the expectations of simulations and models based on the standard ΛCDM cosmology and on the extension of the star formation efficiency measured at lower redshifts (e.g., M. Castellano et al. 2022, 2023; S. L. Finkelstein et al. 2023, 2024). Many physical interpretations of such a tension have been discussed in the literature. Among these, the feedback-free regime at high z (e.g., A. Dekel et al. 2023), top-heavy stellar initial mass function (e.g., A. Trinca et al. 2024), negligible dust attenuation (e.g., A. Ferrara 2024a), and stochastic star formation (C. A. Mason et al. 2023; A. Kravtsov & V. Belokurov 2024) constitute viable astrophysical explanations.

While all the above solutions concern the complex physics relating star formation to the evolution of dark matter (DM) haloes at high redshifts, there are hints that the problem may be rooted in the cosmological framework. For example, the large number density of massive galaxies already in place at such large redshifts (e.g., I. Labbé et al. 2023; M. Xiao et al. 2023; C. M. Casey et al. 2024) seems to be on the verge of challenging the ΛCDM models even assuming a maximal efficiency $\epsilon = 1$ for the conversion of baryons into stars at earlier epochs (e.g., N. Menci et al. 2022; M. Boylan-Kolchin 2023; C. C. Lovell et al. 2023). Although the stellar mass estimates of these galaxies are uncertain and even their identification is subject to debates (R. Endsley et al. 2023; D. D. Kocevski et al. 2023; K. Chworowsky et al. 2024), confirmation of such results would imply the need for a revision of the cosmological model. In particular, the abundance of such galaxies might be easily accounted for by assuming a dynamical (i.e., time-evolving) DE equation of state parameter $w = p/\rho$ characterized by *phantom* behavior $w < -1$ at early epochs, and a larger value $w > -1$ at present times (N. Menci et al. 2022).

What makes such an explanation particularly interesting is that recent measurements from independent cosmological probes concur in indicating that the problem may be rooted in the DE sector of the current cosmological scenario. In fact, recent breakthroughs from baryonic acoustic oscillations (BAO) measured by the Dark Energy Spectroscopic Instrument (DESI; DESI Collaboration et al. 2024) collaboration, when combined with the cosmic microwave background (CMB) observations by Planck and with the luminosity distance measurements through Type Ia Supernovae (SNIa) have shown deviations from the ΛCDM predictions (within a two-parameter DE model) estimated as 2.5σ, 3.5σ, and 3.9σ depending on the supernova data set included in the compilation (respectively, PantheonPlus, Union3, and DESY5). Although these results depend on a particular kind of parameterization for the evolution of DE, the hint of phantom crossing in the DE equation of state has also been inferred for different DE parameterizations (K. Lodha et al. 2024; W. Giarè et al. 2024) as well as with model-independent analysis (R. Calderon et al. 2024). The same phantom behavior of DE has also been shown to constitute a possible explanation of the JWST observations of massive galaxies at $z \gtrsim 6$ (see N. Menci et al. 2022; M. Cortês & A. R. Liddle 2024).

While the above measurements strongly suggest that the expansion history of the Universe differs from that envisaged by the concordance ΛCDM cosmological model, a DE equation of state with $w < -1$ is extremely problematic for all the scenarios in which the cosmic acceleration is traced back to the dynamics of a scalar field ϕ. In all these scenarios a scalar field ϕ rolling in a potential $V(\phi)$ would yield an equation of state parameter $w = (\dot{\phi}^2 - V(\phi))/(\dot{\phi}^2 + V(\phi))$. While such

scenarios are attractive because—for a proper form of the potential $V(\phi)$—they would provide a natural way to achieve a negative equation of state and an accelerated expansion (in analogy to the mechanism at the basis of cosmic inflation), achieving $w < -1$ would require a negative kinetic term (see K. J. Ludwick 2017, for a review). However, an expansion history consistent with all the observations mentioned above can be achieved considering a field whose potential features a negative minimum (anti-de Sitter (AdS) vacuum). In this case, the positive energy density $\rho_x > 0$ of the evolving DE component on top of a negative cosmological constant (nCC) must yield a net positive value $\rho_x + \rho_\Lambda > 0$ around the present time, so as to be consistent with the observed late-time acceleration.

Such scenarios have been widely investigated in the literature. Besides the solid theoretical motivation for the presence of an nCC (M. Demirtas et al. 2022; S. Antonini et al. 2023), such models have been proved to perform equally well as ΛCDM, or are even potentially statistically preferred, when confronted with a number of cosmological probes (see, e.g., R. Calderón et al. 2021; S. A. Adil et al. 2023; A. A. Sen et al. 2023). In addition, nCC models can help to reduce the well-known 5σ tension between early and late Universe inferences of the Hubble constant H_0 (e.g., Planck Collaboration et al. 2020; A. G. Riess et al. 2022) in the ΛCDM scenario (A. A. Sen et al. 2023). Finally, the nCC scenario provides a better match to the observed abundance of massive galaxies even assuming a quintessence (i.e., nonphantom) DE equation of state (N. Menci et al. 2024).

In this context, here we show that nCC models are also characterized by a boost in the characteristic mass for collapse with respect to ΛCDM that provides a potential cosmological explanation for the observed standstill in the evolution of the bight end of the UV luminosity functions (LFs) at $z > 9$. Although it is perfectly possible that one (or more) of the astrophysical processes described above can be responsible for such observations, it is intriguing that, while the astrophysical processes need to be tuned to modify the galaxy L/M ratios in the redshift range $z \approx 10$–15, nCC models provide a natural way to account for such a standstill in this redshift range, without the need for sharp changes in the physics of galaxy formation.

2. DE Models with nCC

A feature common to most scalar field DE models is the positivity of the ground state of the field potential $V(\phi)$, corresponding to a stable or meta-stable de Sitter (dS) vacuum. In the simplest model, the scalar field ϕ is settled at this minimum, resulting in a positive cosmological constant that can drive the accelerated expansion of the Universe. A more general scenario is when the field ϕ is not settled at the minimum of $V(\phi)$ but rolls slowly over the potential and we get a dynamical DE, popularly termed as "quintessence." Unfortunately, constructing such a quintessence field with a dS ground state is extremely challenging in quantum gravity theories. In fact, according to swampland conjecture, a dS ground state, or at least a stable dS ground state, cannot appear in any reliable string theory construction, see C. Vafa (2005) and P. Agrawal et al. (2018). On the other hand, a scale field rolling over a potential with negative minimum (also known as AdS minimum or ground state) is a common feature in string theory; one of the reasons being the famous AdS/conformal field theory (AdS-CFT) correspondence (J. M. Maldacena 1999) as well as due to holography (M. Van Raamsdonk & C. Waddell 2024a). AdS ground state for scalar field potentials results in the presence of a negative cosmological constant, and using scalar fields with such potentials having AdS minimum is a perfectly viable model for quintessence.

Motivated by the above considerations, here we study some striking implications of such quintessence models with AdS vacua on galaxy formation. Instead of taking any particular potential for the scalar field (which would restrict us to a specific model), we parameterize the dynamical nature of its equation of state $w(a)$ using the most popular Chevallier–Polarski–Linder (CPL) parameterization, see M. Chevallier & D. Polarski (2001) and E. V. Linder (2003):

$$w(a) = w_0 + (1 - a)w_a, \tag{1}$$

where a is the expansion factor and w_0 and w_a are two arbitrary constants. Scalar field models with potentials having an AdS ground state are represented by a dynamical part ρ_x having an equation of state w given by Equation (1) together with a cosmological constant ρ_Λ, which is negative. Finally, the equation governing the expansion of the Universe in such a model is given by

$$\left[\frac{H(a)}{H_0}\right]^2 = \Omega_m a^{-3} + \Omega_\Lambda + \Omega_x f(a), \tag{2}$$

where $f(a) = a^{-3(1+w_0+w_a)} \exp[-3w_a(1 - a)]$ and $\Omega_m + \Omega_\Lambda + \Omega_x = 1$ due to spatial flatness. In the following, we shall keep the value of the matter density parameter $\Omega_m = 0.31$, with the normalization of the Hubble parameter $H_0 = 67\ \mathrm{km\ s^{-1}\ Mpc^{-3}}$ (e.g., Planck Collaboration et al. 2020).

Thus, the total density parameter of the DE sector is $\Omega_{\rm DE} = \Omega_\Lambda + \Omega_x$. Although Λ itself and therefore Ω_Λ can be negative, the total DE density and therefore $\Omega_{\rm DE}$ have to be positive in order to be able to drive the observed cosmic acceleration at low redshifts and maintain agreement with cosmological observations. There have been number of studies in recent times that shows that such a DE model containing a negative cosmological constant is consistent with different cosmological observations. These include the consistency of this model with CMB (as observed by Planck-2018), BAO (as observed by Sloan Digital Sky Survey (SDSS)) as well as SnIa measurements of Pantheon Sample (A. A. Sen et al. 2023). Subsequently, DE models with negative Λ have been confronted with Pantheon-Plus compilation of the SnIa observations (M. Malekjani et al. 2024), with CMB (Planck 2018)+BAO(SDSS)+Pantheon-Plus+SH0ES (S. A. Adil et al. 2024), with JWST photometric and spectroscopic observations of high redshift galaxies (N. Menci et al. 2024), and more recently, with DESI BAO measurements (H. Wang et al. 2024). Moreover, the possible constraints on DE models with negative Λ from near future Square Kilometre Array mid-observations have also been studied recently (C. B. V. Dash et al. 2024).

3. Method

To explore the impact of assuming negative values of Ω_Λ on galaxy formation, we consider the evolution of the characteristic mass for the collapse of perturbations, defined as the mass $M_c(a)$ at which the rms value of density perturbations equals

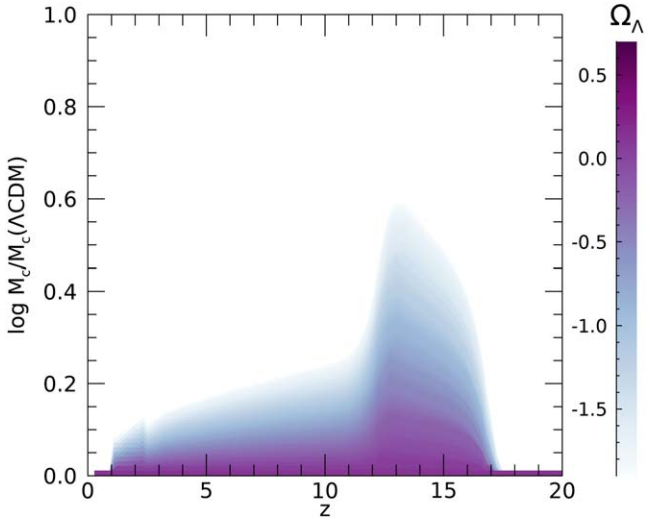

Figure 1. The ratio of the characteristic mass $M_c(t)$ for different nCC models to that in the ΛCDM case, for our fiducial combination $w_0 = -0.9$, $w_a = 0.1$. The color code corresponds to different values of Ω_Λ as shown in the color bar.

the linear density threshold δ_c for collapse, i.e.,

$$\sigma(M_c)D(a) = \delta_c, \tag{3}$$

where $\sigma^2(M)$ is the variance of the linear density field smoothed on the mass scale M, and $D(a) \equiv \delta(a)/\delta(1)$ is linear growth factor $D(a)$ accounting for the evolution of the linear density field δ. This provides the mass at which the exponential factor in any Press and Schechter–like mass distributions of DM halos $dN/dM = e^{-\delta_c^2/2\sigma^2(M)D^2(t))}$ begins to bend down the distribution. In fact, in terms of the characteristic mass, the (W. H. Press & P. Schechter 1974) mass function can be written as $N(M) = \sqrt{(2/\pi)}A\ \rho\ M_c^{-2}(M/M_c)^{A-2}\ exp[-(M/M_c)^{2A}/2]$, where $A = (n_{\rm eff}+3)/6$, and $n_{\rm eff}$ is the effective spectral index of density perturbations at the mass scale M.

Assuming a CDM form for $\sigma(M)$ (J. M. Bardeen et al. 1986), we can derive the characteristic mass M_c after Equation (1) for any nCC cosmology by computing the growth factor of density perturbations $D(a)$. This is obtained by numerically solving the equation governing the linear growth of density perturbations (see S. A. Adil et al. 2023):

$$\delta'' + \left[\frac{3}{a} + \frac{E'(a)}{E(a)}\right]\delta' = \frac{3}{2}\frac{\Omega_m}{a^5E^2(a)}\delta, \tag{4}$$

where indicates a derivative with respect to the scale factor a, and $E(a) \equiv H(a)/H_0$ denotes the normalized expansion rate.

The evolution of the characteristic mass is shown in Figure 1 for cosmological models with different values of the vacuum energy density parameter Ω_Λ. The case with $\Omega_\Lambda = 0.7$ corresponds to the standard ΛCDM cosmology. In all cases, we assume a fiducial combination $w_0 = -0.9$ and $w_a = 0.1$. This is chosen as representative of a nonphantom quintessence behavior for the field responsible for the DE, which is also consistent with the most recent DESI data (see DESI Collaboration et al. 2024). We discuss below how assuming different combinations (w_0, w_a) affects our results.

The striking feature in Figure 1 is the boost in $M_c(z)$ compared to the ΛCDM case for $10 \lesssim z \lesssim 15$. This coincides with the redshift range where current observations are showing an exceeding large abundance of bright galaxies compared to theoretical models and to extrapolations of the LF measured at lower redshifts (e.g., S. L. Finkelstein et al. 2024). The effect of such a boost on the DM mass function is illustrated in Figure 2, where we compare the evolution of the ΛCDM Press and Schechter mass function with the corresponding evolution in three selected nCC models with $\Omega_\Lambda = -0.7$, $\Omega_\Lambda = -0.5$, and $\Omega_\Lambda = -0.2$ (the combination (w_0, w_a) is left fixed to our fiducial values). While at $z = 7$ the effect of assuming nCC cosmologies is negligible, at redshift $z \gtrsim 10$ the DM halo mass function gets a significant boost, whose magnitude grows with progressively smaller (more negative) values of Ω_Λ.

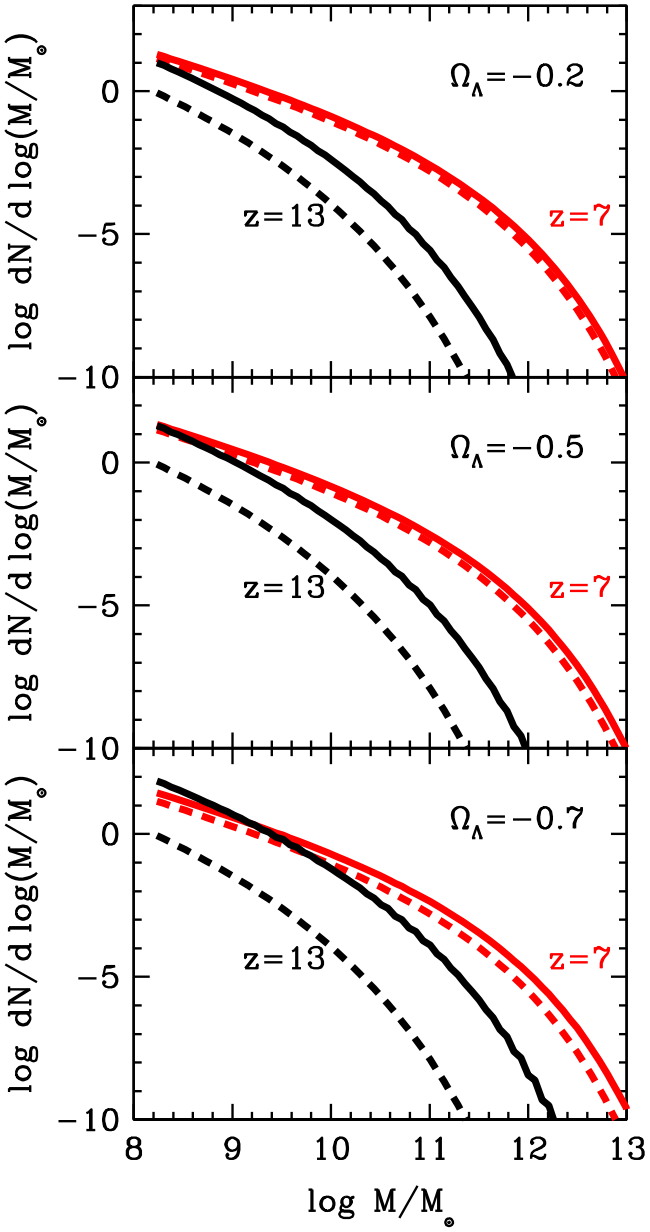

Figure 2. The DM halo mass function corresponding at redshift $z = 7$ (red lines) and $z = 13$ (black lines) in nCC models with different, negative values of Ω_Λ are shown as continuous lines. For reference, we also show as dashed lines the halo mass function corresponding to the standard ΛCMD cosmology.

The physical origin of such a boost is rooted in the dependence of the growth rate of perturbations $D(a)$ on the expansion factor $H(a)$. In fact, a faster expansion inhibits the growth of density perturbations, due to the larger dilution of density perturbations (see, e.g., Equation (2)). Thus, the

dependence of $H(a)$ on the assumed cosmology (see Equation (1)) critically affects the growth factor. At very early times $a \to 0$ the strong dependence of the term related to matter density $\Omega_m a^{-3}$ dominates over all other terms, so that $H(a)$—and hence a characteristic mass $M_c(a)$—is almost independent on the other cosmological parameters Ω_Λ and Ω_ϕ (as shown by the converging behavior of $M_c(z)$ for $z \gtrsim 14$ in Figure 1). However, at lower redshifts, the larger values of a allow the value of Ω_Λ to appreciably affect $H(a)$; Equation (1) shows that for decreasing values of Ω_Λ (and particularly for negative values) a smaller expansion rate $H(a)$ is obtained, resulting into larger growth factors. This explains the increase of $M_c(a)$ compared to the ΛCDM case corresponding to the bump in Figure 1. Finally, for $a \to 1$ the evolution of the expansion rate in Equation (1)—and hence the growth factor $D(a)$, and the characteristic mass $M_c(a)$—reduces exactly to the ΛCDM case (since $\Omega_x + \Omega_\Lambda = 1 - \Omega_m \approx 0.7$; see Section 2).

To test whether such a boost is quantitatively able to account for the observations, we compute the LFs corresponding to nCC cosmologies. We start from the mass function $dN(M)/dM$ of DM haloes in nCC cosmologies, computed for different values of Ω_Λ following the lines in N. Menci et al. (2022). The DM mass M is then related to the star formation rate of galaxies $\dot{m}_* = \epsilon(M) f_b \dot{M}$. Here f_b is the cosmic baryon fraction, and the efficiency $\epsilon(M)$ for the conversion of baryons into stars is taken from C. A. Mason et al. (2015; see their Figure 3). This is a redshift-independent relation characterized by a maximal efficiency at masses $M \approx 10^{12} M_\odot$, and constitutes a phenomenological representation of our knowledge about galaxy formation before the JWST era.

The star formation rate is related to the UV luminosity L through the relation $\dot{m}_*/M_\odot \ \mathrm{yr}^{-1} = k_{\rm UV} L/\mathrm{erg\ s^{-1}\ Hz^{-1}}$ with $k_{\rm UV} = 0.7\ 10^{-28}$ (P. Madau & M. Dickinson 2014), so that $L \propto \epsilon(M)\dot{M}$. The galaxy LFs are then computed as $\phi(L) = dN(M)d\dot{M}/dL$.

Adopting the above efficiency $\epsilon(M)$ to relate the DM mass and the UV luminosity results in a UV LF that captures the evolution of the observed LF over all available observations for $0 \leqslant z \leqslant 10$. It is also consistent with the LF observed by JWST for all redshifts $z \lesssim 9$ (see, e.g., V. Gelli et al. 2024), while it underpredicts the abundances of bright galaxies measured by JWST at higher redshifts. Its behavior is described by a Schechter form $\phi(L) = \phi_*(L/L_c(a))^\alpha \exp(-L/L_c(a))$, where the normalization ϕ_*, the logarithmic slope α, and the evolution of the characteristic luminosity $L_c(a)$ are given in C. A. Mason et al. (2015) for the ΛCDM case. When nCC cosmologies are assumed, the characteristic luminosity L_c gets a boost over the value in the ΛCDM case. A simple estimate of such a boost can be derived by noticing that in the mass range $M \approx 10^9 - 10^{12} M_\odot$ relevant to the high-redshift galaxies considered here, the behavior of $\epsilon(M)$ yields the approximate relation $L/L_\odot \propto (M/M_\odot)^{3/2}$ (see Figure 1 in C. A. Mason et al. 2015). In this case, the LF $\phi(L)$ in nCC can be derived from that given in C. A. Mason et al. (2015) simply by boosting the characteristic luminosity by a factor $L_c/L_c(\Lambda\mathrm{CDM}) \approx [M_c/M_c(\Lambda\mathrm{CDM})]^{3/2}$, where $M_c/M_c(\Lambda\mathrm{CDM})$ is the boost in the characteristic mass shown in Figure 1. In the redshift range $11 \lesssim z \lesssim 15$ a boost in M_c of a factor up to ≈4 thus results in luminosities exceeding the ΛCDM expectations by factors up to ≈8.

Finally, we take into account that observed LFs are usually derived assuming volumes V and luminosity distances D_L inferred assuming the ΛCDM model. Thus, we convert our LFs to the value that they would have when interpreted by an observer that assumes a ΛCDM cosmology, by multiplying the model LF and luminosities by a factor $f_{\rm Vol} = (dV/dz)/(dV_{nCC}/dz)$ and $f_{lum} = D_L^2/D_{nCC}^2$, respectively.

4. Results

In Figure 3 we show the resulting evolution of the LFs for cosmological models with different values of Ω_Λ and for our fiducial choice of the combination (w_0, w_a). While for $z \lesssim 10$ the LFs obtained for different values of Ω_Λ do not show large differences compared to the ΛCDM case (the black line), at larger redshifts the boost in the mass distribution shown in Figures 1 and 2 brings the LFs in much better agreement with data, without changing the star formation prescription with respect to that holding at lower redshifts. Notice that at redshifts larger than $z = 16$ the effect of assuming nCC cosmologies becomes negligible, and the LFs of all nCC models become similar to that predicted in the ΛCDM case. This is a direct consequence of the behavior of the characteristic mass shown in Figure 1, as explained in Section 3, and constitutes a clear prediction of our study that can be tested with future results from JWST.

The corresponding evolution of the luminosity density of the whole galaxy population is shown in Figure 4, and compared with different data sets. While a detailed best-fit approach is beyond the demonstrative scope of this paper, we notice that the values of Ω_Λ, which provide a good match to the observed LFs and to the luminosity density in all redshift bins, can be qualitatively estimated as $\Omega_\Lambda \approx (-0.6, -0.3)$. It is extremely interesting that such a range of values is close to the preferred range of Ω_Λ obtained from the analysis of the recent DESI data when Ω_Λ is allowed to vary (H. Wang et al. 2024). This is particularly noticeable since in principle Ω_Λ can take any value.

Figure 4 clearly enlightens the sharp prediction of nCC models discussed above, namely, the fast decline of the boost in mass and luminosity with respect to ΛCDM predictions for $z \gtrsim 15$, where the evolution of the LFs and luminosity density of the Universe are expected to merge with that envisaged by ΛCDM. This behavior constitutes a clear way to disentangle the cosmological effects considered here from the astrophysical processes, which might also affect the evolution of the LFs at early epochs.

Finally, we notice that our conclusions do not depend on our specific choice of a fiducial combination (w_0, w_a). Indeed, we show in Figure 5 the effect of varying the (w_0, w_a) combination on the values of Ω_Λ, which provide (within 5% accuracy) the same boost in the maximum characteristic mass (and hence the same LFs) of our fiducial choice. It is seen that, within the constraints on (w_0, w_a) provided by current DESI+Planck +SNIa data, values $\Omega_\Lambda \approx (-0.6, -0.3)$ are obtained. Remarkably, this is consistent with that obtained from the analysis of DESI data in the overlapping region of the (w_0, w_a) plane (H. Wang et al. 2024).

5. Discussion

In this paper, we propose that two ground-breaking recent observational results—the indications for evolving DE resulting from combined cosmological probes, and the excess of bright sources at high redshifts $z \gtrsim 10$ compared to pre-JWST expectations—stem from a unique cosmological origin, tracing

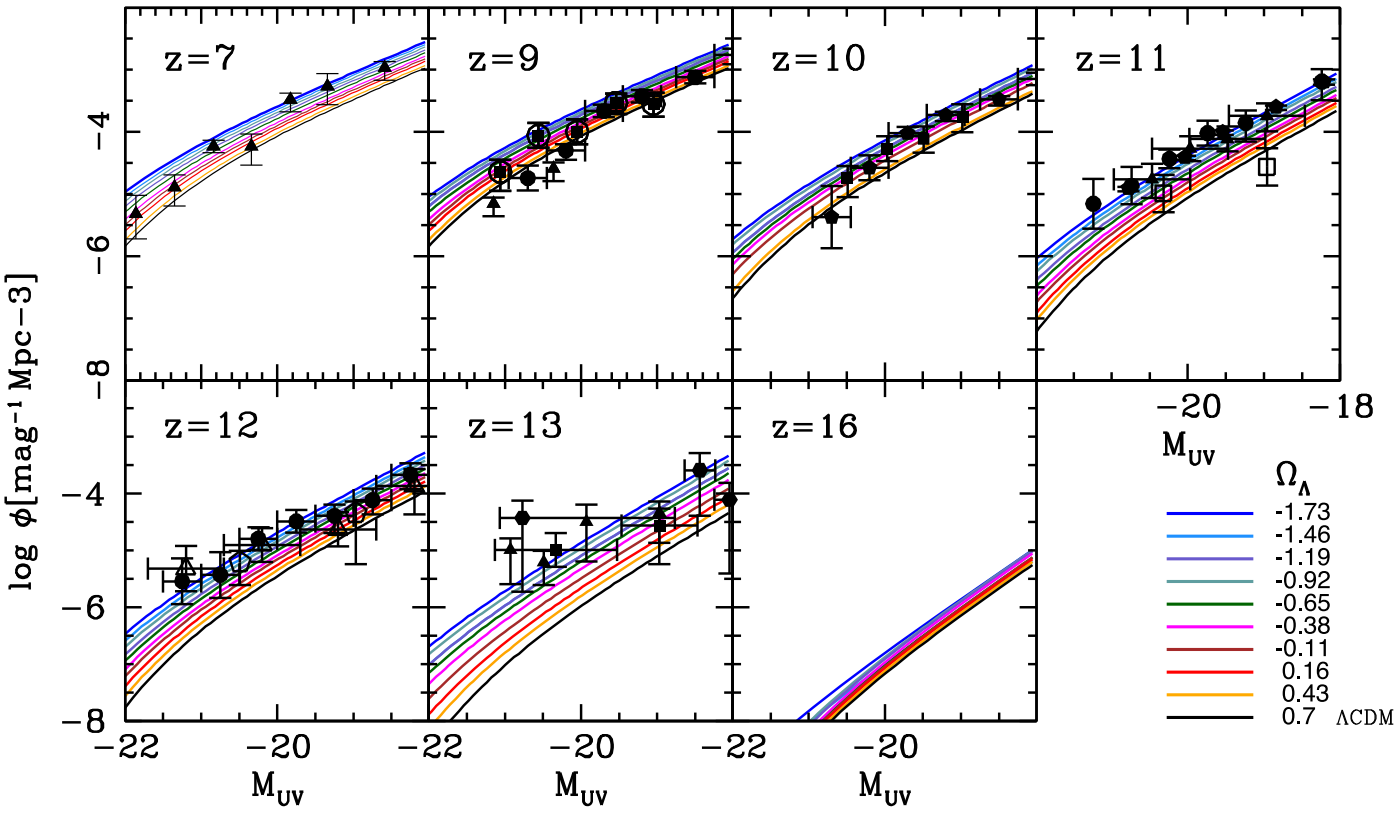

Figure 3. The evolution of galaxy LFs for the different values of Ω_Λ shown in the legend. We assumed our fiducial choice of the combination $w_0 = -0.9$ and $w_a = 0.1$. The data are from R. J. Bouwens et al. (2015, 2021, 2022) (filled triangles), S. L. Finkelstein et al. (2023) (filled squares), M. Stefanon et al. (2021) (open circles), C. T. Donnan et al. (2023) (filled circles), D. J. McLeod et al. (2024) (filled pentagons), C. M. Casey et al. (2024) (empty squares), Y. Harikane et al. (2023) (empty triangles), N. J. Adams et al. (2024) (empty pentagons), and B. Robertson et al. (2024) (filled hexagons).

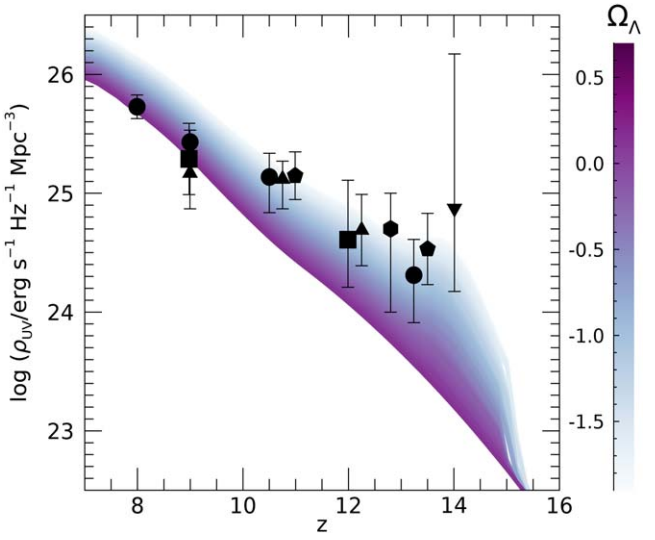

Figure 4. The evolution of UV luminosity density for the values of Ω_Λ shown in the color bar, and for our fiducial combination $w_0 = -0.9$ and $w_a = 0.1$. The data are from S. L. Finkelstein et al. (2023) (downward triangles), C. T. Donnan et al. (2024) (circles), D. J. McLeod et al. (2024) (filled pentagons), Y. Harikane et al. (2023) (squares), N. J. Adams et al. (2024) (hexagons), and P. G. Pérez-González et al. (2023) (upward triangles).

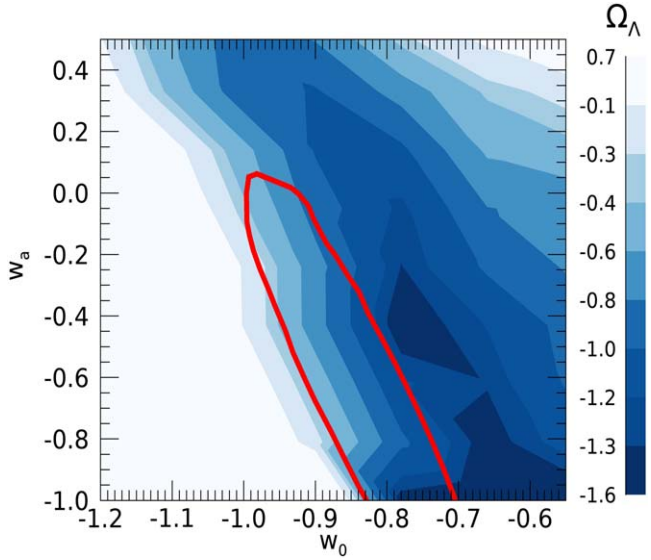

Figure 5. For each (w_0, w_a) we show as colored contours the values of Ω_Λ leading to the same boost (to within 5%) in the peak value of the characteristic mass shown in Figure 1. The red contour shows the 2σ confidence region consistent with CMB+DESI+Pantheon Plus data sets (H. Wang et al. 2024).

back to a DE with negative Λ. Here we discuss the robustness of the two observational results above and their different interpretations in the literature.

The strong ($\sim 3.9\sigma$) evidence for DE is based on the combination of BAO and Planck observations with the Dark Energy 5 yr (DES5Y) SN sample. While recent works have raised the possibility of an incorrect calibration for this sample (G. Efstathiou 2024), tensions at the level of (or larger than) $\sim 2.5\sigma$ persist when different SNe samples (PantheonPlus and Union3) are considered. While the assumption of CPL parameterization may indeed affect the conclusions, it is

interesting to note that the region of the parameter space (w_0, w_a) favored by the above combined cosmological probes is also favored by the observations of massive galaxies at redshifts $z \approx 6$–9 (N. Menci et al. 2024) and that 2σ indications for dynamical DE also result when BAO compilations from the completed SDSS are adopted as late-time cosmological observables (U. Mukhopadhayay et al. 2024). In addition, independent analysis (see, e.g., M. Van Raamsdonk & C. Waddell 2024b) prior to the last DESI results considered different time-changing $w(a)$ beyond the CPL approximation (in particular, linear potential models), also found dynamical DE solutions to be favored compared to ΛCDM.

As for the recent estimates of the UV LF, the excess of bright sources compared to pre-JWST expectations has been shown on the basis of spectroscopic follow-up to be robust against potential systematics in target selection and redshift uncertainties (e.g., Y. Harikane et al. 2024b), and it is unlikely explained by cosmic variance effects being found at high-significance in several, independent survey fields (e.g., D. J. McLeod et al. 2024). A possible explanation could reside in the contribution of active galactic nuclei (AGN) to the UV emission of high redshift galaxies (e.g., S. Hegde et al. 2024), but this would require black holes overmassive with respect to their host galaxies compared to the local relation (in the specific redshift range $z \gtrsim 10$). Although it has been suggested that this might indeed be the case at high redshifts (see R. Maiolino et al. 2024), in current samples the majority of the detected objects have extended morphologies, suggesting that an AGN is not the dominant source of luminosity (e.g., Y. Harikane et al. 2024a).

On the other hand, several physical scenarios have been proposed potentially producing a slower evolution of the UV LF that either require peculiar, short-lived evolutionary phases or a sudden change in the underlying star formation processes. It has been suggested that the high UV luminosities highlight an increase in the star formation efficiency at high redshift (e.g., S. L. Finkelstein et al. 2024), which in turn may be due to the occurrence of feedback-free starbursts, i.e., efficient star formation on timescales shorter than the typical timescale to develop winds and SNe (A. Dekel et al. 2023). As an alternative, it has been suggested that the slow evolution of the UV LF beyond $z \sim 9$ is explained by strong radiation-driven outflows in a short-lived, high specific star formation rate "super-Eddington phase," which clears the objects from the previously formed dust (F. Fiore et al. 2023; A. Ferrara 2024a, 2024b). A similar boosting effect on the UV LF may result from an increased stochasticity of the star formation histories at very high redshift (e.g., C. A. Mason et al. 2023; A. Kravtsov & V. Belokurov 2024). However, recent efforts to include such effects in cosmological semianalytic models of galaxy formation (L. Y. A. Yung et al. 2024) have failed to account for the observed excess even assuming dust-free models. For example, they showed that the inclusion of stochastic bursts of star formation would require a rather large stochastic component ($\sigma_{\rm UV} \approx 2$, where $\sigma_{\rm UV}$ is the root variance of a Gaussian random deviation in UV magnitude) to account for the observed excess. This is much larger than the stochasticity produced in the high-resolution radiation-hydrodynamic cosmological simulations of A. Pallottini & A. Ferrara (2023), which yield typical $\sigma_{\rm UV} \approx 0.6$. Notice that such models do not include any suppression of star formation by the UV background at $z \gtrsim 8$, yet they still underpredict the observed counts. Thus, the proposal that the observed excess could be explained by the lack of suppression of star formation via photoionization before reionization seems also to fail in providing a complete explanation of the observations. Other recent studies of galaxy formation in a cosmological context based on hydrodynamic simulation report basically the same conclusions, see, e.g., X. Wu et al. (2020) and R. Kannan et al. (2023).

Finally, more mundane explanations rely on an increased UV luminosity due to the presence of emission from Population III stars or AGN (Y. Harikane et al. 2023), or a top-heavy initial mass function (A. Trinca et al. 2024). While all the above-mentioned scenarios provide viable astrophysical explanations for the measured excess in the UV LF, they postulate a somewhat sudden change in the galaxy properties or physical processes in the first ∼500 Myr after the Big Bang. In the present work, we have shown that the boosting effect on DM masses due to a negative Λ yields UV LFs that are compatible with recent estimates without requiring any modification in the underlying baryonic processes. Other explanations that have been proposed that do not postulate a substantial change in galaxy formation processes propose an enhancement of the power spectrum on scales of ∼1 Mpc (H. Padmanabhan & A. Loeb 2023; see also Parashari and Laha 2023), a different time-redshift relation (F. Melia 2023, 2024), or an accelerated formation of galaxies and clusters in MOND cosmologies (S. S. McGaugh et al. 2024). However, such alternatives at the moment are either based on ad hoc modifications of some cosmological quantities or lack a comprehensive theoretical framework of the underlying physical mechanisms. Compared to the theoretical works mentioned above, the agreement between the range of values for Ω_Λ needed to match the observed LFs in nCC cosmologies discussed in the present paper and that obtained from independent cosmological probes provides a tantalizing perspective. In addition, the cosmological scenario we propose allows us to simultaneously account not only for the recent DESI results and for the observed abundance of UV luminous galaxies at $z \gtrsim 10$, but also for the unexpectedly large number of massive galaxies at $z \gtrsim 6$ and observational results that are now being confirmed by spectroscopic data and which, although marginally consistent with ΛCDM predictions, appreciably favors phantom models (N. Menci et al. 2022), or models with nCC (N. Menci et al. 2024).

In this context, disentangling between phantom and nCC models is not an easy task. In fact, as noted in the Introduction, phantom models also simultaneously account for the same wide set of observations. On the one hand, on the theoretical side, phantom models are difficult to justify in terms of fundamental physics (see Section 1), while AdS vacua are ubiquitous features of holographic scenarios for gravity and string models. On the other hand, on the observational side, the sudden drop in the abundance of luminous galaxies shown in Figures 3 and 4 constitutes a clear prediction of nCC models in the context of the CPL parameterization. However, Y. Tada & T. Terada (2024) have shown that the $w_0 - w_a$ parameter space for CPL parameterization as constrained by DESI observations can be mapped to a quintessence scalar field with a potential having a negative or AdS minimum. Thus, a more rigorous approach toward disentangling between the two cosmological scenarios will necessarily require an analysis beyond the CPL parameterization, and approach we plan to take on in forthcoming works.

Future efforts aimed at discriminating among the above-mentioned scenarios will need to be based on a multifaceted approach. The models postulating a change in galaxy evolution processes at $z \gtrsim 9$ will need to be tested through a detailed measurement of their predictions on galaxy properties such as metallicity, specific star formation rate, gas conditions, dust obscuration, and prevalence of AGN emission. On the other hand, a promising way to discriminate among various scenarios is to test predictions on the abundance of bright galaxies at earlier epochs. Pushing the constraints on the UV LF at $z \gtrsim 15$ is challenging, albeit within reach of JWST instruments (C. J. Conselice et al. 2024). In this respect, as shown in the present work, galaxy evolution in nCC cosmologies presents a very clear prediction of a sharp decrease in galaxy abundance at redshifts higher than those probed so far.

6. Conclusions

Motivated by recent breakthroughs in cosmology resulting from combined cosmological probes, we have considered the effect of assuming cosmological models with a DE sector containing a negative Λ as a ground state of the quintessence field on the galaxy LF at high redshifts. Our main results can be summarized as follows.

1. The DM masses of galaxies in the redshift range $10 \lesssim z \lesssim 15$ are boosted with respect to the ΛCDM expectations by a factor 2–4 depending on the value of Ω_Λ. This approximately corresponds to a boost in UV luminosity $\approx M^{3/2} \approx 3$–$8$ (see discussion at the end of Section 3).
2. When luminosities are related to the DM mass using standard relations that proved to match to the LFs at lower redshifts, the boost in the DM mass characterizing nCC models yields LFs that are able to match the LFs observed by JWST for $10 \lesssim z \lesssim 15$, without the need to implement new physics to relate DM mass to the star formation. The sensitivity of the LFs to the value of Ω_Λ makes them a valuable tool for measuring such a quantity.
3. The range of values $\Omega_\Lambda = [-0.6, -0.3]$ needed to match the observed LFs at $10 \lesssim z \lesssim 15$ in nCC cosmologies agrees with that obtained from the combined analysis of the recent DESI data with existing independent cosmological probes.
4. nCC models thus affect the UV luminosities in the right redshift range needed to match the JWST observations, and with the correct value of Ω_Λ, which is required by independent cosmological probes (H. Wang et al. 2024).
5. A sharp prediction of nCC models for the evolution of the LFs and luminosity density of the Universe is the sharp decline of the boost in mass and luminosity with respect to ΛCDM predictions at epochs earlier than $z \approx 15$. This behavior constitutes a clear way to disentangle the cosmological effects considered here from the astrophysical processes, which might also affect the evolution of the LFs at early epochs.

Acknowledgments

We acknowledge support from the INAF Mini-grant "Reionization and Fundamental Cosmology with High-Redshift Galaxies" and from the INAF Theory-grant "AGN-driven outflows in cosmological models of galaxy formation." A.A.S. acknowledges the funding from SERB, Govt. of India under the research grant No. CRG/2020/004347. A.A.S. also acknowledges support from INAF—Osservatorio Astronomico di Roma, Rome, Italy; CERN, Switzerland; and Abdus Salam International Centre For Theoretical Physics, Trieste, Italy, for his visits where part of the work has been done. We thank the referee for the useful comments that helped to improve the manuscript.

ORCID iDs

N. Menci https://orcid.org/0000-0002-4096-2680

References

Adams, N. J., Conselice, C. J., Austin, D., et al. 2024, ApJ, 965, 169
Adil, S. A., Akarsu, Ö., Di Valentino, E., et al. 2024, PhRvD, 109, 023527
Adil, S. A., Mukhopadhyay, U., Sen, A. A., & Vagnozzi, S. 2023, JCAP, 2023, 072
Agrawal, P., Obied, G., Steinhardt, P. J., & Vafa, C. 2018, PhLB, 784, 271
Antonini, S., Simidzija, P., Swingle, B., & Van Raamsdonk, M. 2023, PhRvL, 130, 221601
Bardeen, J. M., Bond, J. R., Kaiser, N., & Szalay, A. S. 1986, ApJ, 304, 15
Bouwens, R. J., Illingworth, G. D., Oesch, P. A., et al. 2015, ApJ, 803, 34
Bouwens, R. J., Illingworth, G. D., van Dokkum, P. G., et al. 2022, ApJ, 927, 81
Bouwens, R. J., Oesch, P. A., Stefanon, M., et al. 2021, AJ, 162, 47
Boylan-Kolchin, M. 2023, NatAs, 7, 731
Calderón, R., Gannouji, R., L'Huillier, B., & Polarski, D. 2021, PhRvD, 103, 023526
Calderon, R., Lodha, K., Shafieloo, A., et al. 2024, JCAP, 2024, 048
Casey, C. M., Akins, H. B., Shuntov, M., et al. 2024, ApJ, 965, 98
Castellano, M., Fontana, A., Treu, T., et al. 2022, ApJL, 938, L15
Castellano, M., Fontana, A., Treu, T., et al. 2023, ApJL, 948, L14
Chevallier, M., & Polarski, D. 2001, IJMPD, 10, 213
Chworowsky, K., Finkelstein, S. L., Boylan-Kolchin, M., et al. 2024, AJ, 168, 113
Conselice, C. J., Adams, N., Harvey, T., et al. 2024, arXiv:2407.14973
Cortês, M., & Liddle, A. R. 2024, MNRAS, 531, L52
Dash, C. B. V., Sarkar, T. G., & Sen, A. A. 2024, MNRAS, 527, 11694
Dekel, A., Sarkar, K. C., Birnboim, Y., Mandelker, N., & Li, Z. 2023, MNRAS, 523, 3201
Demirtas, M., Kim, M., McAllister, L., Moritz, J., & Rios-Tascon, A. 2022, PhRvL, 128, 011602
DESI Collaboration, Adame, A. G., Aguilar, J., et al. 2024, arXiv:2404.03002
Donnan, C. T., McLeod, D. J., McLure, R. J., et al. 2023, MNRAS, 520, 4554
Donnan, C. T., McLure, R. J., Dunlop, J. S., et al. 2024, MNRAS, 533, 3222
Efstathiou, G. 2024, arXiv:2408.07175
Endsley, R., Stark, D. P., Whitler, L., et al. 2023, MNRAS, 524, 2312
Ferrara, A. 2024a, A&A, 684, A207
Ferrara, A. 2024b, A&A, 689, A310
Finkelstein, S. L., Bagley, M. B., Ferguson, H. C., et al. 2023, ApJL, 946, L13
Finkelstein, S. L., Leung, G. C. K., Bagley, M. B., et al. 2024, ApJL, 969, L2
Fiore, F., Ferrara, A., Bischetti, M., Feruglio, C., & Travascio, A. 2023, ApJL, 943, L27
Gelli, V., Mason, C., & Hayward, C. C. 2024, ApJ, 975, 192
Giarè, W., Najafi, M., Pan, S., Di Valentino, E., & Firouzjaee, J. T. 2024, JCAP, 2024, 035
Harikane, Y., Inoue, A. K., Ellis, R. S., et al. 2024a, arXiv:2406.18352
Harikane, Y., Nakajima, K., Ouchi, M., et al. 2024b, ApJ, 960, 56
Harikane, Y., Ouchi, M., Oguri, M., et al. 2023, ApJS, 265, 5
Hegde, S., Wyatt, M. M., & Furlanetto, S. R. 2024, JCAP, 2024, 025
Kannan, R., Springel, V., Hernquist, L., et al. 2023, MNRAS, 524, 2594
Kocevski, D. D., Onoue, M., Inayoshi, K., et al. 2023, ApJL, 954, L4
Kravtsov, A., & Belokurov, V. 2024, arXiv:2405.04578
Labbé, I., van Dokkum, P., Nelson, E., et al. 2023, Natur, 616, 266
Linder, E. V. 2003, PhRvL, 90, 091301
Lodha, K., Shafieloo, A., Calderon, R., et al. 2024, arXiv:2405.13588
Lovell, C. C., Harrison, I., Harikane, Y., Tacchella, S., & Wilkins, S. M. 2023, MNRAS, 518, 2511
Ludwick, K. J. 2017, MPLA, 32, 1730025
Madau, P., & Dickinson, M. 2014, ARA&A, 52, 415
Maiolino, R., Scholtz, J., Curtis-Lake, E., et al. 2024, A&A, 691, A145

Maldacena, J. M. 1999, AIPC, 484, 51
Malekjani, M., Mc Conville, R., O Colgain, E., Pourojaghi, S., & Sheikh-Jabbari, M. M. 2024, EPJC, 84, 317
Mason, C. A., Trenti, M., & Treu, T. 2015, ApJ, 813, 21
Mason, C. A., Trenti, M., & Treu, T. 2023, MNRAS, 521, 497
McGaugh, S. S., Schombert, J. M., Lelli, F., & Franck, J. 2024, ApJ, 976, 13
McLeod, D. J., Donnan, C. T., McLure, R. J., et al. 2024, MNRAS, 527, 5004
Melia, F. 2023, MNRAS, 521, L85
Melia, F. 2024, A&A, 689, A10
Menci, N., Adil, S. A., Mukhopadhyay, U., Sen, A. A., & Vagnozzi, S. 2024, JCAP, 2024, 072
Menci, N., Castellano, M., Santini, P., et al. 2022, ApJL, 938, L5
Mukhopadhayay, U., Haridasu, S., Sen, A. A., & Dhawan, S. 2024, arXiv:2407.10845
Padmanabhan, H., & Loeb, A. 2023, ApJL, 953, L4
Pallottini, A., & Ferrara, A. 2023, A&A, 677, L4
Parashari, P., & Laha, R. 2023, MNRAS: Lett., 526, L63
Pérez-González, P. G., Costantin, L., Langeroodi, D., et al. 2023, ApJL, 951, L1
Planck Collaboration, Aghanim, N., Akrami, Y., et al. 2020, A&A, 641, A6
Press, W. H., & Schechter, P. 1974, ApJ, 187, 425
Riess, A. G., Yuan, W., Macri, L. M., et al. 2022, ApJL, 934, L7
Robertson, B., Johnson, B. D., Tacchella, S., et al. 2024, ApJ, 970, 31
Sen, A. A., Adil, S. A., & Sen, S. 2023, MNRAS, 518, 1098
Stefanon, M., Bouwens, R. J., Labbé, I., et al. 2021, ApJ, 922, 29
Tada, Y., & Terada, T. 2024, PhRvD, 109, L121305
Trinca, A., Schneider, R., Valiante, R., et al. 2024, MNRAS, 529, 3563
Vafa, C. 2005, arXiv:hep-th/0509212
Van Raamsdonk, M., & Waddell, C. 2024a, arXiv:2406.02688
Van Raamsdonk, M., & Waddell, C. 2024b, JCAP, 06, 047
Wang, H., Peng, Z.-Y., & Piao, Y.-S. 2024, arXiv:2406.03395
Wu, X., Dave, R., Tacchella, S., & Lotz, J. 2020, MNRAS, 494, 5636
Xiao, M., Oesch, P., Elbaz, D., et al. 2023, arXiv:2309.02492
Yung, L. Y. A., Somerville, R. S., Finkelstein, S. L., Wilkins, S. M., & Gardner, J. P. 2024, MNRAS, 527, 5929